EFFECT OF LINE INTERFERENCE ANO FINITE DURATION OF COLLISIONS ON THE MOLECULAR ABSORPTION SPECTRA

M.V. Tonkov and N.N. Filippov

Scientific Research Institute of Physics
at the Leningrad State University
Received April 25, 1990

Effect of line interference and finite duration of molecular collisions on the IR gas spectra is considered. An overview of experimental studies of this effect is presented and its theoretical description is given. It is demonstrated that line interference considerably redistribute the intensities in the region of overlapping lines including a *sharp decrease of the absorption in the band edges. The effect of finite duration of collisions plays an important role in forming the far wings of the bands.*

INTRODUCTION

One of the principal factors which has an appreciable effect on the extinction of IR radiation during its propagation through the atmosphere is the molecular absorption. To calculate it exactly, in addition to the frequencies and intensities of the rovibrational lines (the data on these parameters can be found in the well-known atlases[1–3]), one needs a developed theory for describing the rovibrational band shapes in molecular spectra. Historically for a long time theoretical studies of line shapes were based on experimental investigations of the atomic spectra (Lorentz, Yablonskii, and Weiskopf). This fact stimulated a development of the theoretical branches which dealt with the description of the band center (the model of the Lorentz line shape) and with the use of the adiabatic approximation and perturbation theory for numerically calculating the wings of the lines.

Since the 1950's the theory of molecular spectra stimulated has been developing apace by the advances in the experimental methods and the well-known Anderson[4] study. These investigations have shown that in the bands with high resolution of rotational structure at pressures of a gas which exceed several millimeters of mercury, the central parts of the line shapes are adequately described by the Lorentz line shape with the line width being linearly dependent on the gas density. Anderson's theory and its subsequent versions and modifications[5–7] made it possible to perform a quantitative analysis of the coefficients of line broadening.

However, the success of these theoretical studies to a strong degree, was provided by their use for calculating atmospheric transparency. The problem is that a complete absorption is observed in the centers of the lines of the principal atmospheric components. Meanwhile, the propagation of the IR radiation through the so-called atmospheric transparency windows is determined by the line shape near the wing of the lines. At the same time the indicated theoretical approach contains a number of approximations which restrict its application for describing the wings of the lines. First limitation is caused by the use of collisional or Markovian approximation in which we ignore the effects of finite duration of collisions. As we will show, this approach results in errors in the computed line shape near the line edge when the displacement with respect to the line center exceeds the inverse duration of a collision. The second limitation inherent to the molecular spectra is caused by the representation of the band by isolated noninteracting lines. The fact that we ignore the line interaction may lead to the errors in describing those spectral regions, where two or more lines make comparable contributions to the total absorption. Such regions are, in particular, the regions of the wings of the overlapping lines. In the paper we consider a theoretical approach which permits us to avoid these two limitations and to analyze the relative contribution of these effects to the formation of different parts of the line shape. The developed approach is used also for quantitative results.

GENERAL FORHALISM

TBe line shape in the IR absorption spectrum can be described by the expression

$$A(\omega) = \frac{4\pi^2(\omega + \omega_v)}{3hc}\left\{1 - \exp\left[-h\beta(\omega + \omega_v)\right]\right\}\Phi(\omega), \quad (1)$$

where $\beta = (\kappa T)^{-1}$, κ is the Boltzmann constant, T is the gas temperature, ω is the cyclic frequency of displacement with respect to the band center,

$$\Phi(\omega) = \pi^{-1}\mathrm{Re}\int_0^\infty dt\, e^{-i\omega t}C(t) \quad (2)$$

is the spectral function, $C(t)$ is the correlation function of the vector M of the dipole moment of the corresponding vibrational transition, and ω_V is the vibrational transition cyclic frequency.[8,11] The term nearly the spectral function in Eq. (1) is of versatile character, so that in analysis of the band shapes it is expedient to concentrate our attention on the properties of the spectral function (2). Formula (1) was obtained on the assumption that the rovibrational interaction affects insignificantly the considered band shape. As the first approximation, the effect of weak rovibrational interactions is to be accounted for by introducing corrections to the line cyclic frequencies.

For simplicity, let us consider a system consisting of spectroscopically active molecule A and the surrounding particles which play the role of a bath. The Hamiltonian of this system can be represented in the form $H = H_A + H_B + H_1 = H_0 + H_1$, where H_A is the rotational Hamilltonian of the molecule A, H_B is the bath Hamiltonian, and H_1 is the term

0235-6880/91/02 95-16 $02.00

describing the perturbation of rotational movement of the molecule due to its surroundings. In analyzing the correlation and spectral functions, it is convenient to employ the formalism of the line space.[6,9–10] Each operator P from the state space is relevant for a vector $|P\gg$ in the line space. The scalar product of such vectors is the thermodynamic average of the product of relevant operators

$$\ll P|Q\gg = \mathrm{Sp}(\rho P + Q) \text{ and } \rho = e^{-\beta H}/\mathrm{Sp}\left[e^{-\beta H}\right].$$

On the basis of this formalism, the correlation function acquires the form

$$C(t) = \ll M|\exp(-iLt)|M\gg ,$$

where $L = L_0 + L_1$ is the Liouvillian of the system $L_1 P \gg \hbar^{-1}\ [H_1, P]\gg$. The vector $|M\gg$ from the line space can be represented as the expansion in orthonormal vectors[6] $|m\gg$, which are the eigenvectors of the Liouvillian L_Λ: $L_\Lambda |m\gg \omega_m |m\gg$ and

$$|M\gg = |M|\sum_m C_m |m\gg, \text{ and } \sum_m |C_m|^2 = 1.$$

Hereafter the dipole moment is scaled to the condition $|M|^2 = 1$.

The use of the kinetic approach for constructing the correlation function allows us to derive the expression for the spectral function (2)[12–15]

$$\Phi(\omega) = \pi^{-1}\mathrm{Re}\ll M|[i(\omega - L_\Lambda) + \Gamma(\omega)]^{-1}|M\gg = \pi^{-1}\mathrm{Re}\sum_{mm'} C_m^* C_{m'} \ll m|[i(\omega - L_\Lambda) + \Gamma(\omega)]^{-1}|m'\gg , \quad (3)$$

where $\Gamma(\omega)$ is the generalized (cyclic frequency dependent) relaxation operator somet1mes called the memory operator.[16] As can be seen from Eq. (3), the properties of the spectral function, which depend on perturbation, are determined by the operator $\Gamma(\omega)$. Let as consider two of the most popular approximations of this operator.

In the first approximation (the model of the isolated lines) we ignore all the nondiagonal matrix elements of the relaxation operator.[17] On the basis of this model, we obtain from Eq. (3)

$$\Phi(\omega) = \pi^{-1}\sum_m |C_m|^2 \frac{\Gamma'_{mm}(\omega)}{[\omega - \omega_m + \Gamma''_{mm}(\omega)]^2 + [\Gamma'_{mm}(\omega)]^2},$$

i.e., the spectral function does simply become a sum of the line shapes centered in the vicinity of cyclic frequencies of the corresponding radiative transitions.

$$\Gamma'_{mm'}(\omega) = \mathrm{Re}\ll m|\Gamma(\omega)|m'\gg,$$

and

$$\Gamma''_{mm'}(\omega) = \mathrm{Im}\ll m|\Gamma(\omega)|m'\gg.$$

In the second approximation, we ignore the spectral dependence of the $\Gamma(\omega)$ operator.[13–15,18–19] The characteristic cyclic frequency scale, for which the matrix elements of the above operator significantly change, is determined by the va1ue τ_k^{-1}, where τ_k is the correlation time of rotational perturbations of the molecule (the duration of collisions). Therefore, within the cyclic frequency interval $\Delta\omega$, which satisfies the condition

$$\Delta\omega \ll \tau_k^{-1}, \quad (5)$$

the variations in $\Gamma_{mm'}(\omega)$ can be neglected. This approximation is more often employed for not too high gas pressures to describe the central parts of lines. In this case when the cycle frequency displacements with respect to the line center satisfy the condition $|\omega - \omega_m| \lesssim |\Gamma_{mm}(\omega)| \ll \tau_k^{-1}$, the value of $\Gamma_{mm}(\omega)$ can be substituted by $\Gamma_{mm}(\omega_m)$ in Eq. (4). Hence it follows that the central parts of lines in Eq. (4) have the Lorentz line shapes with the halfwidths $\Gamma'_{mm}(\omega_m)$. The aim of Anderson' s theory and its modifications[4–7] is to calculate these values. The aim of Anderson' s theory and its modifications[4–7] is to calculate these values. If collisions are nonadiabatic,

$$\omega_R \ll \tau_k^{-1}, \quad (6)$$

where $\omega_R = \left(\sum_m |C_m|^2 \omega_m^2\right)^{1/2}$ is the rms cyclic frequency of rotational transitions in the given band of the molecule A (the characteristic gap between the most populated rotational energy levels), we can ignore the spectra1 dependence of the relaxation operator in the centra1 part of the band up to its wings assuming (the Markovian approximation) and set

$$\Gamma(\omega) = \Gamma(0) \equiv \Gamma. \quad (7)$$

When the model of isolated lines is used together with the Eq. (7), the spectral function acquires the form of a sum of the Lorentz components not only in the region of the central parts of the lines, but in the region of their wings as well

$$\Phi(\omega) = \Phi_{Lor}(\omega) = \pi^{-1}\sum_m |C_m|^2 \frac{\Gamma'_{mm}}{(\Delta\omega_m + \Gamma''_{mm})^2 + (\Gamma'_{mm})^2}. \quad (8)$$

Hence it follows that the observed deviations of the line shapes from the sum of the Lorentz curves indicate that either one or both of the employed approximations are incorrect. Let us now consider which deviations from the Lorentz line shape are to be expected when we abandon either the approximation of the isolated lines or the Markovian approximation. At the first stage Eq. (6) is assumed to be satisfied, so that the spectral dependence of the $\Gamma(\omega)$ operator can be ignored in the considered spectral region, while the deviations from line shape (8) are caused by the line interactions.

SPECTRAL EFFECTS OF INTERFERENCE

The line interaction (interference) can be il1ustrated by the following example. Let the investigated particle be the oscillator capable of existence in one of the two possible states which differ in oscillation cyclic frequencies (the four-level system[20]). Let us assume that mean free time for collisions that entail changes in the molecular states is connected with the oscillation cyclic frequencies via the relationship, $\tau_f^{-1} \ll \omega_2 - \omega_1 \ll \omega_1$. The dependence $M(t)$ and the corresponding spectra1 function are shown in Fig. 1*a*. The two lines with high resolution are observed in the spectrum, the central parts of these lines are described by the Lorentz line shape with halfwidth τ_f^{-1}, which increases with collision frequencies.[20] In the region of the line wings of the Lorentz character of the dependence is destroyed, it is of the super-Lorentz character in the troughs between the lines and of the sub-Lorentz character region in the far wings.

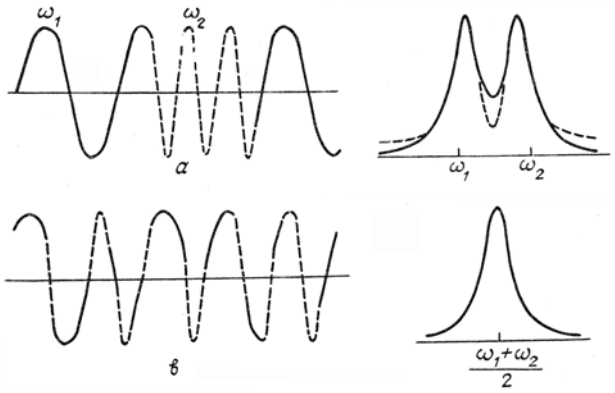

FIG. 1. Temporal evolution of *the dipole moment and the spectral function shape. The dashed shape is the sum* of *the Lorentz components extrapolated from the center* of *lines.*

As τ_f decreases in the region

$$\tau_f^{-1} \gg \omega_2 - \omega_1, \tag{9}$$

the dependence $M(t)$ becomes close to periodic with an average cyclic frequency $\omega_0 = (\omega_1 + \omega_2)/2$, and the spectral function then describes a single line centered at a cyclic frequency ω_0 with the linewidth which decreases with increase of the collision cyclic frequency.[20] The dependence $M(t)$ and the line spectral shape for this case are shown in Fig. 1*b*. The phenomenon of narrowing the spectrum (collapse) for strong overlapping line is one of the effects of line interference. It has been observed in numerous experiments.[21–23] The intensity redistribution in the region of wings of the overlapping lines is an initial stage of this phenomenon.

It was demonstrated in Ref. 24 that in order a collapse take place, the relaxation operator should have an eigenvector with zero eigenvalue. For purely rotational collisional perturbations the vector $|M\gg$ from the line space[10 15] turns out to be appropriate vector, i.e., for any $|P\gg$ the equality

$$\ll P|\Gamma(\omega)|M\gg = \ll M|\Gamma(\omega)|P\gg = 0, \tag{10}$$

is satisfied[15].

These expressions can be represented as a double-summation rule for matrix elements of the relaxation operator

$$\sum_m \Gamma_{m',m}(\omega)\, C_m = \sum_{,m} \Gamma_{m',m}(\omega)\, C_m^* = 0. \tag{11}$$

The summation rule (11) determines main salient features of the interference effect. They can be formulated as follows.

1. The effect of line interference is manifested in the region of strong overlapping lines, including the overlapping wings.

2. Line interference results in redistribution of the intensities in the band, in addition the intensity of central parts of the band (the region of relatively strong lines) rises due to its edge.

To describe the effect of line interference, various models are used for the relaxation operator.[10,25–29] The simplest convenient model for the qualitative analysis of the interference effect is the model of strong collisions. According to this model, the transition probability of the molecule to fixed rotational state due to collision is independent of the initial state of molecule and is described by the thermal distribution. On the basis of this model, the matrix elements of the relaxation operator have the form[10]

$$\Gamma_{m',m} = \tau_f^{-1}\left(\delta_{m',m} - C_{m'} C_m^*\right), \tag{12}$$

i.e., contain only one parameter — the collision frequency τ_f^{-1}, which can be determined from the well–known average of line coefficient broadening in the band and from the gas pressure.[20] The use of Eq. (12) makes it possible to derive the analytic expression for the spectral function of the band

$$\Phi(\omega) = \pi^{-1}\mathrm{Re}\,\frac{S(\omega)}{1 - \tau_f^{-1} S(\omega)},$$

which does not contain any adjustable parameters, where

$$S(\omega) = \sum_m \frac{|C_m|^2}{i\Delta\omega_m + \tau_f^{-1}}.$$

We shall start our review of experimental studies of line interference in the IR gas spectra with strong overlapping lines. Similar effects have been thoroughly studied as applied to the bands of isotropic Raman scattering,[22,23] in which strong line overlapping is achieved at relatively low gas pressures. Line overlapping in the IR bands of elementary molecules is usually attained at pressures of a few tens of atmospheres. Figure 2 is shows the observed line shape of the $2\nu_1 + \nu_3$ band of CO_2 in a mixture of CO_2 and Ar at gas pressure $P = 94$ atm and for a temperature of 273 K.[30] The same figure shows the line shape which is a superposition of the Lorentz line shapes perfectly with halfwidths $P\gamma_m$, where γ_m is the experimentally determined coefficient of line m broading at relatively low gas pressures. The observed deviations of the band shape from the sum of the Lorentz line shapes perfectly correspond to the expected properties of interference effects. Computer calculations performed in Ref. 30 using the model of strong collisions with the parameter $\tau_f^{-1} = P\sum_m |C_m|^2 \gamma_m$ describe fairly well the experimentally observed line shapes (Fig. 2).

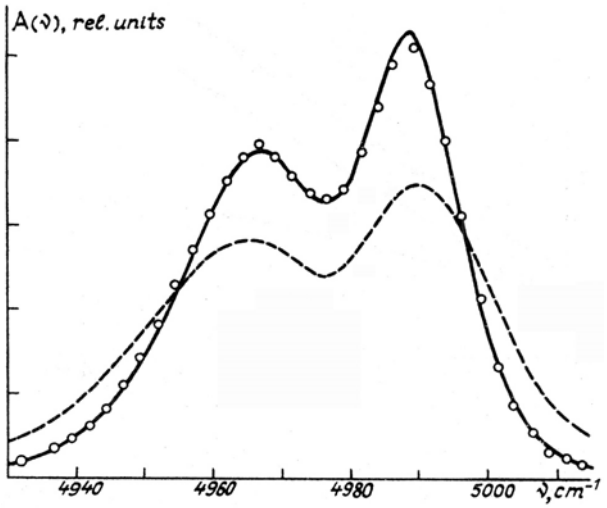

FIG. 2. The shape of the $2\nu_1 + 2\nu_3$ *band of* CO_2 *in a mixture of* CO_2 *and* Ar. *Circles stand for experimental results of Ref. 30. The computational results are shown by the dashed curve for the sum of the Lorentz line shapes and by the solid curve for the model of strong collisions.*

In a number of IR bands of the elementary molecules there are groups of close lines, which overlap at pressures close to atmospheric pressure. These region involve the bands near their edges and the *Q*–branches of the bands. The part of the $3\nu_3$ band of CO_2 near its edge in a mixture of CO_2 and He was

investigated in Refs. 31–33. It was shown from a comparison of the observed absorption with the computational results obtained under the assumption of the Lorentz line shape that the computer line shapes agree fairly well with the measured one in the region of the highly resolved lines $R(22)$–$R(34)$. However, the measured absorption exceeds computed one in the narrow region of close overlapping lines $R(36)$–$R(42)$. This excess absorption increases with gas pressures. Immediately behind the line $R(40)$ with the highest frequency a sharp transition to the sub–Lorentz line shape is observed in Fig. 3. A similar effect is observed in the mixture of CO_2 and N_2 at atmospheric and higher pressures[31–32] The deviations of the line shape of the sub–Lorentz character were discovered for this system at atmospheric pressure in Ref. 33. The model of the strong collisions provides qualitative description of indicated deviations from the Lorentz line shape. However, it predicts an appreciably less effect. The observed deviations from the model line shape near the band edge can be described successfully using a more flexible model,[31,32] where the adjustable parameter is the number of the adjacent lines which take part in the interactions, while the summation rule (11) still holds.

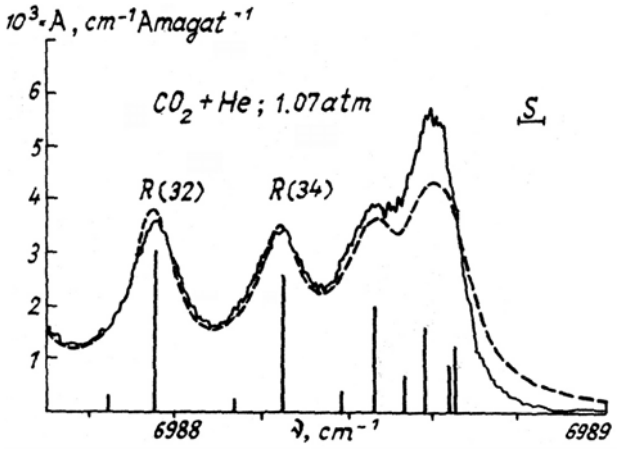

FIG. 3. Absorption in the $3\nu_3$ band of CO_2 near its edge for $T = 291$ K. The solid curve is for experimental results[31,32] and the dashed curve stands for the sum of[the Lorentz lines. Vertical bars show the line center positions and relative intensities, the horizontal bar shows the spectral slit width used for measurements.

Individual lines in the Q–branches and near the edge of the bands are close one to another and not equidistant. At low gas densities they follow the Lorentz line shape. When the gas density rises, the closest 1ines start to overlap. These lines correspond to the transitions with low values of angular momentum. In these regions the line shape cannot be described by the sum of the Lorentz lines.[34,35] At the initial stage the number of lines which follow condition (9) is small in comparison with the total number of lines in the band, and the shape of the Q–branch appears to be close to that found in the spectra of isotropic Raman scattering.[36] It was this fact that made the description of the shape of IR spectrum successful[35] by applying the computational models developed for the isotropic Raman scattering.[37] The same approach was used in Ref. 25.

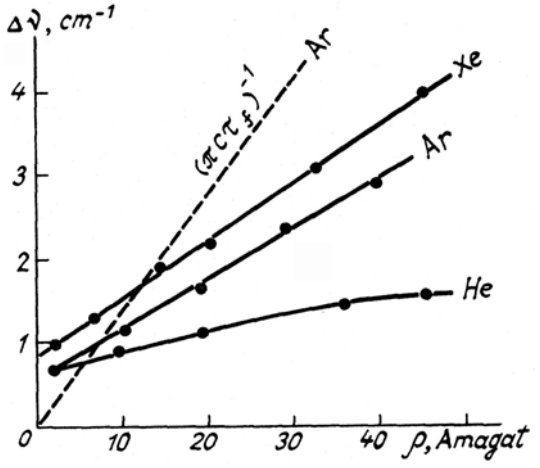

FIG. 4. The width $\Delta\upsilon$ of the Q–branch of the $\upsilon_1 + \upsilon_2$ band of CO_2 for $T = 292$ K. Points show the experimental results of Ref. 38. Dashed straight line shows the average line width in the P– and R–branches in a mixture of CO_2 and Ar.

When condition (9) is satisfied for all the lines of the Q–branch, the band of the isotropic spectrum of Raman scattering which consists of the single Q–branch enters into the state of collapse.[22,23] However, the line overlap in the Q–branch of the IR absorption spectrum does not imply overlapping of all the interacting lines in the band necessary for starting the stage of line narrowing, since the lines of the P– and R–branches start to overlap only at much higher pressures. That is why the Q–branches in the IR absorption bands continue to broaden after complete overlapping of all the lines. However, the rate of broadening becomes much slower than the rate of line broadening prior to the line overlap as well as the rate of broadening of lines in the P– and R–branches. Figure 4 shows the data of Ref. 38. It demonstrates the dependence of the Q–branch width on pressure for the $\nu_1 + \nu_2$ band (near 2076 cm^{-1}) of CO_2 in a mixture of CO_2 and different buffer gases. As can be seen from this figure, the Q–branch width increases slower than the average line width of the P– and R–branches. At some moment the lines of these two bands get wider than the entire width of the Q–branch. One of such spectra is shown in Fig. 5. As in the case of the band near its , edge, the model of strong collisions provides qualitatively correct description of this effect but results in underestimation of its expected value (Fig. 5). The structure of the relaxation matrix, which enables one to interpret the experimental data, has been calculated theoretically in Ref. 29 for a mixture of CO_2 and He. The calculations indicate that interaction between the lines of different branches is much weaker than the interaction between the lines of one and the same branch. The weaker the interaction of the lines of the Q-branch with the lines of the P– or R–branches, i.e., the lower the relative value of the relevant elements of the relaxation matr1x $\Gamma_{mm'}$, the slower is the broadening of the Q–branch. In the hypothetical limiting case, in which there are no Q–P and Q–R interactions (the model of the isolated branch) after complete overlap of lines, the Q–branch should enter into a stage of line narrowing similar to that in the bands of isotropic Raman scattering.

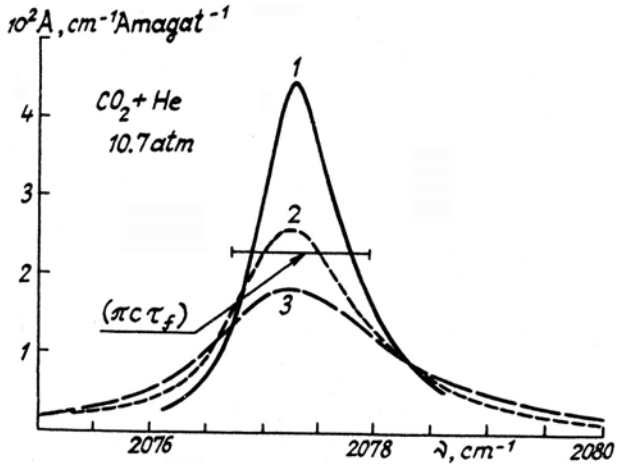

FIG. 5. The shape of the Q–branch of the $\nu_1 + \nu_2$ *band of* CO *for* 292 K *at* P = 10.7 atm. *Experimental data are borrowed from Ref.* 38:
1) *experiment. Computational results:*
2) *superposition of the Lorentz line shape;* 3) *model of strong collisions.*

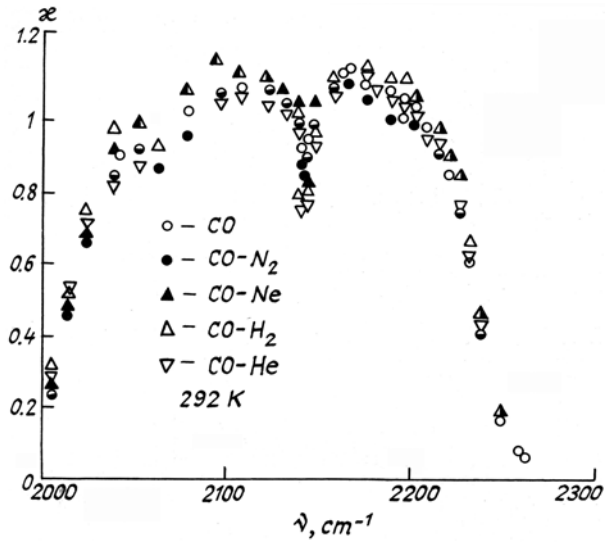

FIG. 6. Observed deviations of the band shape from the superposition of the Lorentz line shapes in the atmospheric transparency microwindow centers of the 1–0 band of CO *in pure gas and different gas mixtures.*[10]

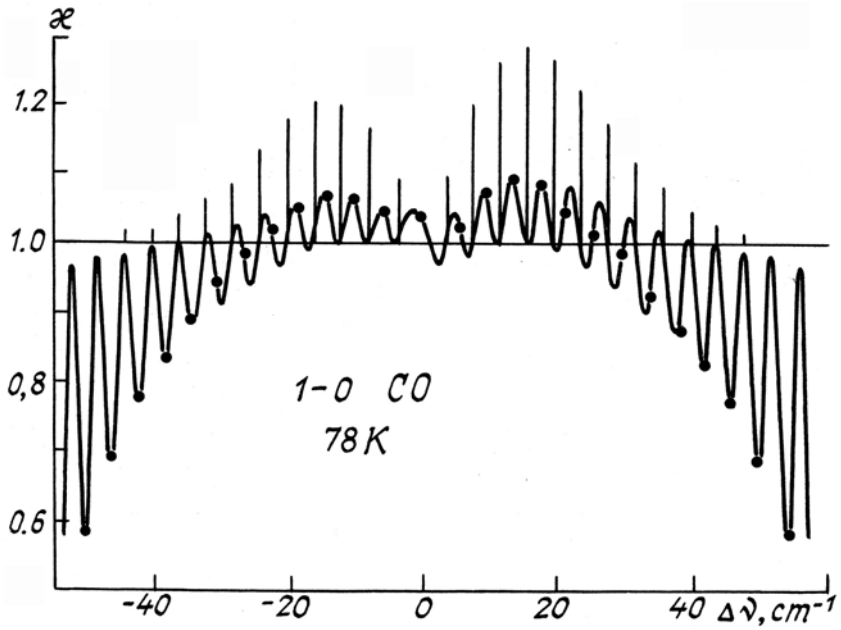

FIG. 7. Profile of the adjustable function of a band computed following the model of strong collisions. Points indicate values of the adjustable function at the atmospheric transparency microwindow centers, and $\Delta\upsilon$ *is the displacement with respect to the band center.*

An increase of absorption by strong lines caused by interference due to absorption in the bands near their edges can be observed at low gas pressures when the line widths are much smaller than the line separation. This effect is observed in the troughs between the lines (in the atmospheric transparency microwindows)[10,26,39,40] and in the far wings of the lines which form the wing of the band. The non–Lorentz character of absorption in these regions can be conveniently characterized by the adjustable funct1on of the band

$$\kappa(\omega) = \Phi(\omega) / \Phi_{Lor}(\omega).$$

The data that have been obtained in Ref. 10 for band of fundamental tone of CO in mixtures of CO and different buffer gases[10] indicate a weak dependence of the values $\kappa_{exp} = \Phi_{exp} / \Phi_{Lor}$ on the nature of perturbing particles (Fig. 6) including such particle characteristics as mass and, consequently, the duration of collisions. This allow us to consider the band shape in atmospheric transparency microwindows in the Markov approximat1on.

$CO_2 + H_2$

Figure 7 demonstrates the adjustable function for the band of fundamental tone of CO $T = 78$ K computed with the use of the model of strong collisions for low collis1on cyclic frequencies $\tau_f^{-1} \ll |\omega_m - \omega_{m'}|$, where $m \neq m'$. Vertical bars denote the positions and relative intensities of individual lines. An interesting salient feature of the computed function κ is its oscillating character with the oscillation period close to (but not equal to) the separation between the lines in the band. Around the centers of relatively strong lines the funct1on κ becomes unity, $\kappa > 1$ in the troughs between the strong lines, and $\kappa < 1$ in the troughs between the weak lines near the band edge. There can be found atmospheric microwindows in the intermediate region of the band where both the sub– and super–Lorentz parts of the line shapes combine. Figure 8 shows the theoretical and experimental[10] values of κ in the region from the line $R(4)$ to the line $R(10)$ of the principal band of CO in a mixture of CO and H_2. The experimental and computed data agree fairly well.

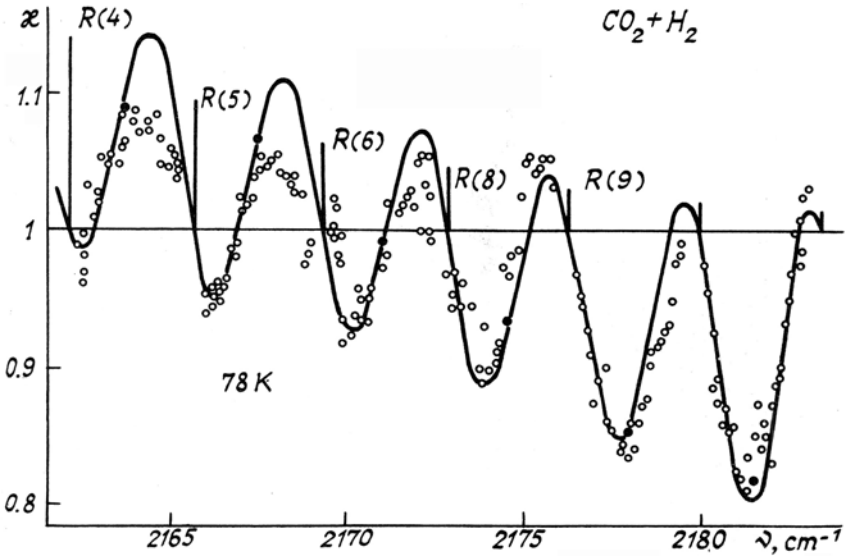

FIG. 8. Adjustable function for the 1–0 *band of* CO *in the troughs between the lines. Empty circles – experiment.*[10] *Filled circles – values of adjustable function at microwindow centers, obtained from the data of the independent measurement series.*[10] *The solid curve shows computational results obtained on the basis of the model of the strong collisions. Vertical bars indicate the line positions and relative intensities.*

In studying absorption in atmospheric transparency microwindows the measurements are performed, as a rule, at the centers of the troughs between the lines. Figure 7 shows the values of the adjustable function at the centers of such microwindows as individual points. As can be seen from this figure, the boundary of the region of transition from the super–Lorentz to the sub–Lorentz absorption, which is found from these data, is located near the boundary of the region of relatively strong lines, so that changes in the width of the rotational structure of the band with temperature of a gas should result in the respective shift of the boundary of transition from super– to sub–Lorentz absorption at the centers of atmospheric microwindows. The experimental studies[10] of the temperature dependence of κ testify to this suggestion (Fig. 9).

The indicated regularities of the IR band shapes in the atmospheric transparency microwindows were also observed in studying the spectra of CO_2 and N_2O.[10,26,39,40] To describe these effects, more realistic empirical computational models were used along with the model of strong collisions[26,39] as well as quantum mechanical computations of the relaxation matrix based on the theoretical values of potential of colliding particles.[27] The values of κ in the atmospheric transparency microw1ndows computed by different methods become close in value. This allowed the authors of Refs. 26 and 27 to make a conclusion that in these spectral regions the value of κ is weakly sensitive to the concrete specific form of the relaxation model used to compute the matrix $\Gamma_{mm'}$. This conclusion is in agreement with the above–mentioned weak effect of the type of perturbing particles on the shape of $\kappa(\omega)$ in the atmospheric transparency microwindows (Fig. 6). This dependence gradually increases in going to the wing of the band, in which the effect of finite duration of collisions might be expected.

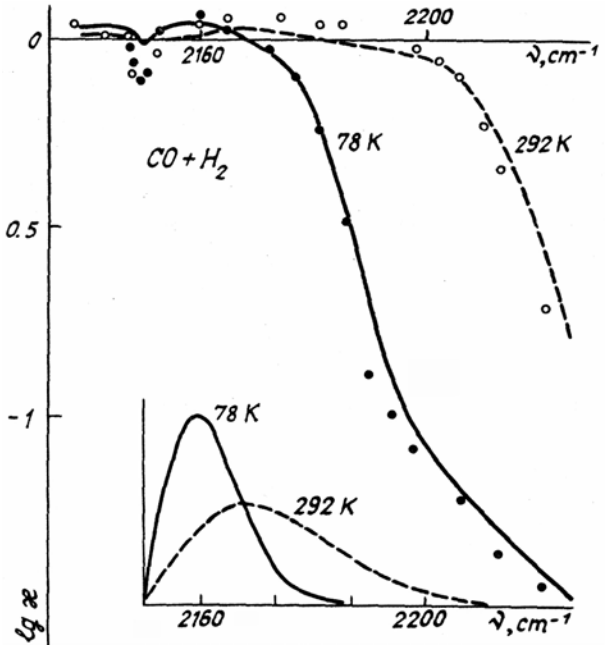

FIG. 9. Temperature dependence of the adjustable function for the 1–0 *band of* CO *at the atmospheric transparency microwindow centers. Empty and filled circles show experimental results of Ref. 10. For clearness, the points computed using the strong collisions model are joined by smooth curves. A diagram of relative line intensities for investigated temperatures is shown below.*

THE EFFECT OF THE FINITE DURATION OF COLLISIONS ON THE SHAPE OF THE WING OF THE BAND

In contrast to the atmospheric transparency microwindows in the central part of the band the absorption in the wings of the band exhibits a well–pronounced dependence on the nature of perturbing particles.[41–49] To describe the band shape in this spectral region, let us now consider the asymptotic form of function (3) for large displacements with respect to the band center

$$|\omega| \gg \omega_R \tag{13}$$

and

$$|\omega| \gg |\Gamma_{mm'}(\omega)|. \tag{14}$$

Representing the operator $\left[i(\omega - L_A) + \Gamma(\omega)\right]^{-1}$ in Eq. (3) in terms of powers of $\omega^{-1}\left[iL_A - \Gamma(\omega)\right]$ we obtain

$$\Phi(\omega) = \pi^{-1}\mathrm{Re}\sum_{n=0}^{\infty}(i\omega)^{-1-n}\langle\langle M|[iL_A - \Gamma(\omega)]^n|M\rangle\rangle$$

Taking into account the double–summation rule (10) and (11), this series to an accuracy of $\sim\omega^{-4}$ has the form

$$\Phi(\omega) = \pi^{-1}\mathrm{Re}\left[-i\sum_{n=0}^{3}\frac{\mu_n}{\omega^{n+1}} + \frac{\langle\langle M|L_A\,\Gamma(\omega)\,L_A|M\rangle\rangle}{\omega^4}\right]. \tag{15}$$

where $\mu_n = \langle\langle M|(L_A)^n|M\rangle\rangle = \sum_m |C_m|^2\omega_m^n$. Since the values μ_n are real, it follows from Eq. (15) that

$$\Phi(\omega) = \pi^{-1}\omega^{-4}\,\mathrm{Re}\langle\langle M|L_A\Gamma(\omega)L_A|M\rangle\rangle . \tag{16}$$

If the condition (5) is satisfied for $|\omega|$ along with the conditions (13) and (14) we may proceed to the Markov approximation in Eq. (16):

$$\Phi(\omega) = \pi^{-1}\omega^{-4}\,\mathrm{Re}\langle\langle M|L_A\Gamma(\omega)L_A|M\rangle\rangle. \tag{17}$$

Expression (17) shows that the asymptotic behavior of the spectral function in the Markov approximation is of the form ω^{-4}. The non–Markovian character of the collisional perturbations should manifest itself in deviations of the band shape from the ω^{-4} dependence in the cyclic frequency region $|\omega| \gtrsim \tau_k^{-1}$.

Starting from the explicit form of the operator $\Gamma(\omega)$, the relation between $\Phi(\omega)$ and the dynamics of binary collisions of an absorbing linear molecule was found in Ref. 15. The same result was obtained in Ref. 49 by the different method. The expression founid in Refs. 15 and 49 acquires the simplest form in the case of nonadiabatic collisions

$$\Phi(\omega) = \frac{2n_p}{I_A\omega^4}\left(1 + \exp(-\hbar\beta\omega)\right)^{-1}F(\omega), \tag{18}$$

which satisfy the condition (6), where

$$F(\omega) = \frac{1}{2\pi}\int_{-\infty}^{\infty} dt\; e^{-i\omega t}\langle N(0)N(t)\rangle_{cl}\ , \tag{19}$$

Starting from the data of theoretical computations of intermolecular potentials,[50–53] the authors of Refs. 15 and 54–56 computed the correlation function of the force moment and its Fourier transform $F(\omega)$ for collisions of the $C0_2$ molecule with He, Ar, and Xe, and for collisions of CO with He and Ar. In calculating it was found that the force moment in these systems is predominantly associated with the short–range repulsive forces, which causes relatively small correlation time of the force moment (duration of collisions), so that the condition of nonadiabaticity (6) is satisfied with an error $\leq 1\%$. The function $F(\omega)$ computed for all the indicated system could be approximated by the expression

$$F(\omega) = \langle N^2\rangle_{cl}\left[2b\omega_k K_1(b)\right]^{-1}\exp\left[-\sqrt{\left(\frac{\omega}{\omega_k}\right)^2 + b^2}\right].$$

where k_1 is the Bessel function and $\omega_k \approx \tau_k^{-1}$ and the values of b are close to unity. It follows from Eq5. (18)–(20) that in the region of the non–Markovian character of perturbations (where the effect of finite duration of collisions manifests itself the Markovian character of the ω^{-4} frequency dependence in the wing of the band is transformed into the dependence of the form $\omega^{-4}\exp(-|\omega|\tau_k)$ if the displacements with respect to the band center satisfy the condition $\omega| \gg \tau_k^{-1}$.

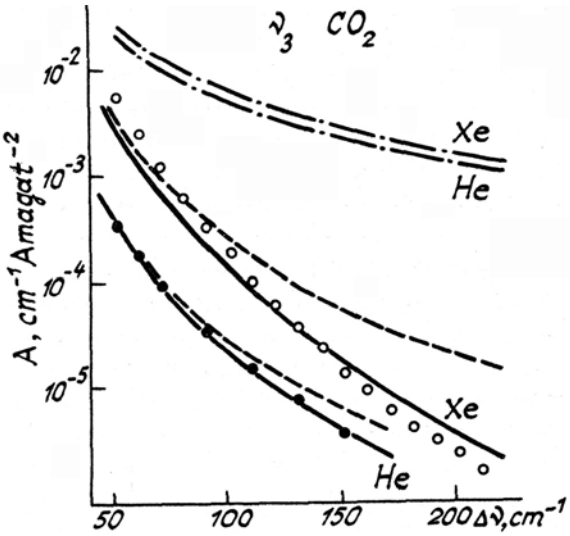

FIG. 10. Absorption in the wing of the ν_3 *band of* CO_2 *in mixtures of* CO_2 *and* He *and* Xe. *Experimental data* are *shown by empty circles for* Xe *for* $T_1 = 291$ K *and by filled circles for* He *for* $T = 295$ K *(Ref.* 47). *Compute calculations are shown by the solid curves for an exact computation, by the dashed curves for the Harkovian approximation, and by the dot–dash curves for the sum of the Lorentz line shapes;* $\Delta\nu$ *is the displacement with respect to the band center.*

Figure 10 shows the calculated results for absorption in the short wavelength wing of the ν_3 band of CO_2 in the mixture of CO_2 and He and Xe in comparison with the experimental data.[48,49] The computations were performed using Eqs. (1), (18) and (20) and the parameters $\langle N^2 \rangle_{cl}$, b, and ω_k in Eq. (20) were found using the potential functions from Refs. 50 and 51. The results of analogous computations for the mixture of CO_2 and Ar, which rely on the potential from Ref. 50 and the experimental data, are presented in Fig. 11. A comparison between the computed and observed values of absorptions indicates a satisfactory agreement between them. The same figures show the shape of the wing of the band computed as a sum of the Lorentz line shapes relevant for the experimental coefficients.

The observed sub–Lorentz character of the absorption in the wing of the bond is caused by not only the finite duration of collisions (the spectral dependence of the function $F(\omega)$ but also the effect of line interference. To demonstrate clearly the relative importance of these two mechanisms. Figs. 10 and 11 show the computational results of the absorpt1on coefficient in the Markovian approximation, i.e., when the function F(ω) is replaced by its value for $\omega = 0$. It is seen from these figures that the factor ω^{-4} in Eq. (18) caused by line interference leads to the deviation of the line shape from the Lorentz line shape by a factor of several tens and several hundreds even neglecting the spectral dependence of the function $F(\omega)$. The effect of finite duration of collisions is manifested in additional deviation of the line shape, whose relative value increases with ω and mass of the perturbing particles.

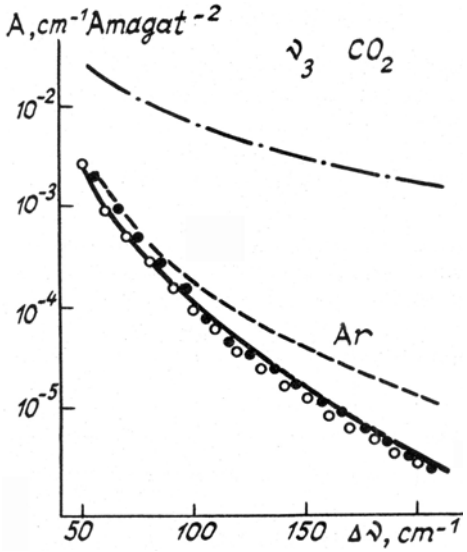

FIG. 11. *Absorption in the wing of the* ν_3 *band* of CO_2 *in a mixture of* CO_2 *and* Ar. *Experimental data are shown by the empty circles for* $T = 290$ K (*Ref.* 48) *and by the filled circles for room temperature (Ref.* 62). *Compute calculations are shown by the curves, see the explanation to Fig.* 10.

Figure 12 shows the computed absorptions in the wing of the band of fundamental tone of CO in mixtures of CO and He and Ar (Ref. 56) and the experimental data that have been obtained in Ref. 47. The experimental data for a mixture of CO and Ar have been obtained here relying on the technique described in Ref. 46. The two potentials of interaction of CO with Ar, which describe fairly well the temperature dependence of the second virial coefficient for the given mixture, are presented in Ref. 52. The correlation part of the potential computed *ab initio* was joined the long–range Van–der–Waals dependence at a point in which their logarithmic derivatives become equal in value. The absolute value of the energy at a point of joining was assumed equal to either the correlation (potential No. 1) or the long–range (potential No. 2) energy.

As can be seen from Fig. 12, the use of potential No. 2 provides fairly good agreement between computed and experimental values of absorption and potential No. 1 underestimates the value of absorption approximately by a factor of two. The result which has been obtained here testifies to a high sensitivity, of absorption in the wing of the band to the form of the potential. Computations with the potential taken from Ref. 53 for the CO + He system allow us to describe correctly the observed spectral behavior in the region of the wing of the band, however, it underestimates the observed value of absorption by a factor of 1.5–2.

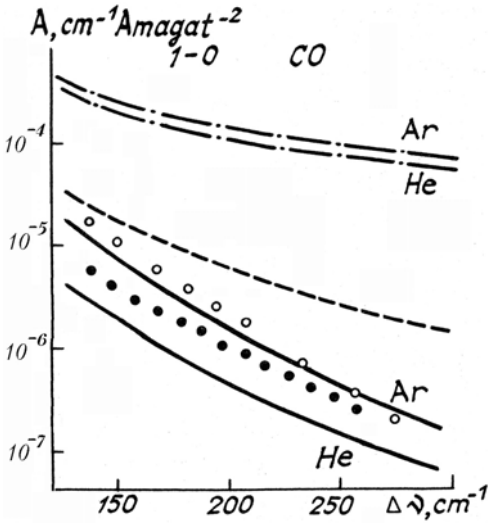

FIG. 12. *Absorption in the wing* of the 1–0 *band of* CO *in a mixture with* He *and* Ar *for* $T = 292$ K. *Experimental data are shown by empty circles for* Ar *and filled circles for* He. *Computations for a mixture of* CO *and* Ar *include the Markov approximation and are shown for potential No.* 2.

As can be seen from Figs. 10–12, the main reason of the sub–Lorentz character of absorption in the near wing of the band for the investigated molecular systems is the line interference. This result explains the success in describing the shape of the central part of the band (up to its near wings) in the Markov approximation. However, absorption in the far wings cannot be described without simultaneous account of the line interference and the finite duration of collisions.

CONCLUSION

Let us now consider the prospects of developing theory of the band shape in the IR absorption spectra of molecular gases. At present the theory of the far wings of the bands along with the theory of line broadening and shifts displacement. The difficulties in the trajectory computations which arise in computing the correlation function of the force moment (or the analogous function in the case of adiabatic collisions[15]) can easily be avoided, viz., by employing the statistical simulation methods.[57]

The theory of the band shape in the region of the central part of the entire band including the regions of overlapping lines and of absorption in the atmospheric transparency microwindows is less developed. First *ab initio* computer calculations of the relaxation matrix[27,29] and the

absorption in the atmospheric transparency microwindows[27] showed that this a problem is at the extreme bounds of capability of modern computers. It seems that in this field one should expect qualitatively new results.

The series of studies[26,31,32,39] should be mentioned here, in which various empirical models of the relaxation matrix are proposed. As a rule, the empirical parameters entering into these models cannot be independently found or used outside the limits of the experiments applied to determine their values. These studies are, undoubtedly, very valuable from the methodological viewpoint since they make it possible to study the relations among the salient features of the relaxation processes, the structure of the relaxation matrix, and the band shape using the models. As for atmospheric applications, such an approach may prove to be useful for approximate description of deformation of the Q–branch shape due to the overlapping lines. However, this approach is too complicated for approximate description of continual absorption in the practical calculations.[40] As it was noted in Ref. 58, for practical purposes a compilation of simple formula of the band shapes along with the values of their parameters is quite sufficient. If qualitative salient features of the band shape are known from experimental studies, the description of the observed continual absorption by the given system with reasonable band shape and two or three adjustable parameters meets with success. An appropriate example of the band shape of this kind is the well–known Benedict band shape.[59]

Line interference and the effect of finite duration of collisions are not the only possible reasons for the found shape deviations from the Lorentz band shape. The deviations can be due to absorption by the dimers and by complexes with more complicated structure of the molecular systems which are capable of generating them.[60] If we are a *priori* aware of the fact that for the conditions of the experiment the investigated molecules have such a capability, we believe that it is incorrect to analyze the band shape without estimating the possible contribution made by dimers. That is why our paper, for which the similar estimates were not the subject of work, has not touched upon the data on the continual absorption in the spectra of water vapor and hydrogen halides. The dimer nature of the absorption may also manifest itself in some of the investigated systems for low temperatures. The estimates of the dimer concentration and contribution to the absorption[10] have demonstrated that the strong super–Lorentz absorption in the troughs between the lines in the central part of the 1–0 band of CO both in pure gas and in a mixture of a gas and N_2 for low temperatures is caused namely was produces by such a dimer mechanism. That is why the analysis of the indicated spectra presented in Ref. 61, which ignore dimmer contribution, must not be considered valid.

REFERENCES

1. R.A. McClatchey, et al., *Atmospheric Absorption Line Parameters Compilation,* Environ. Res. Papers, No. 434, AFCRL–73–0096 (1973).
2. L.S. Rothman, A. Goldman, J.R. Gills, et al., Appl. Opt. **20**, No. 8, 1323–1328 (1981).
3. A. Chedin, N. Husson, and N.A. Scott, The GEISA Data Bank 1984 Version. Laboratoire de Meteorol. Dinamique du CNRS (1986).
4. P.W. Anderson, Phys. Rev. **76**, 647 (1949).
5. C.J. Tsao and B. Curnutte, J. Quant. Spectrosc. Radiat. Transfer **2**, 41–91 (1962).
6. A. Ben–Reuven, Phys. Rev. **141**, 34–40 (1966).
7. D. Rober and J. Bonamy. J. Phys. (Paris) **40**, 923 (1979).
8. R.G. Gordon, Adv. Magn. Reson. **3**, 1–42 (1968).
9. U. Fano, Rev. Mod. Phys. **29**, 74–93 (1957).
10. M.O. Bulanin, A.B. Dokuchaev, M.V. Tonkov, and N.N. Filippov, J. Quant. Spectrosc. Radiat. Transfer **31**, 521–543 (1984).
11. M.A. Yel'yashevich, Atomic and Molecular Spectroscopy (Moscow State Publ. House for Phys. Math. Litr., Moscow, 1962), 892 pp.
12. U. Fano, Phys. Rev. **131**, 259–268 (1963).
13. A. Royer, Phys. Rev. **A6**, 1141–1160 (1972).
14. A. Ben–Reuven, Adv. Chem. Phys. **33**, 235–293 (1975).
15. N.N. Filippov, Mol. Spektrosk., No. 8 (1990).
16. O. Forster, Hydrodynamic Fluctuations, Violated Symmetry, and Correlation Functions (Atomizdat, Moscow, 1980), 288 pp.
17. A. P. Kouzov, Opt. Spektrosk. **49**, 1013–1016 (1990).
18. M. Baranger, Phys. Rev. **111**, 481–504 (1958).
19. A.C. Colb and H. Griem, Phys. Rev. **111**, 514–521 (1958).
20. V.A. Alekseev and I.I. Sobel'man, Zh. Eksp. Teor. Fiz. **55**, 1814–1880 (1968).
21. T.D. Kolomiitsova, S.M. Melikova, and D.N. Shchepkin, Mol. Spektrosk., No. 7, 86-100 (1986).
22. N.S. Golubev, N.D. Orlova, and L.A. Platonova, Pis'ma Zh. Eksp. Teor. Fiz. **35**, 65–68 (1982).
23. N.S. Golubev, N.D. Orlova, and P. Khamitov, Opt. Spektrosk. **62**, 1005–1010 (1987).
24. V.A. Alekseev and A.V. Malyugin, Zh. Eksp. Teor. Fiz. **80**, 897–915 (1981).
25. R.L. Armstrong, Appl. Opt. **21**, 2141–2145 (1982).
26. C. Cousin, H. Le Doucen, C. Boulet, et al., J. Quant. Spectrosc. Radiat. Transfer **36**, 521–538 (1986).
27. J. Boissoles, C. Boulet, D. Robert, and S. Green, J. Chem. Phys. 87, 3436–3446 (1987); ibid, **90**, 5392–5398 (1989).
28. C. Boulet, J. Boissoles, and D. Robert, ibid. **89**, 625–634 (1988).
29. S. Green, ibid. **90**, 3603–3614 (1989).
30. A.A. Yakulin, N.D. Orlova, and V.M. Tarabukhin, Opt. Spektrosk. **60**, 44–48 (1986).
31. I.M. Grigor'ev, V.M. Tarabukhin, and M.V. Tonkov, Opt. Spektrosk. **58**, 244–245 (1985).
32. V.M. Tarabukhin and M.V. Tonkov, Proceedings of the Seventh All–Union Symposium on Molecular Spectroscopy of High and Super–High Resolution, Vol. 3, Tomsk, 1986, pp. 232–236.
33. E.S. Bukova, V.M. Osipov, and V.V. Tsukanov, Atmos. Opt. **2**, No. 3, 267–210 (1989).
34. V.M. Tarabukhin and M.V. Tonkov, Opt. Spektrosk. **62**, 333–335 (1987).
35. L.L. Strow and B.M. Gentry, J. Chem. Phys. **84**, 1149–1156 (1986).
36. B. Lavorel, G. Millot, R. Saint–Loup, et al., J. Phys. **47**, 411–425 (1986).
37. L.A. Rahn, H.E. Palmer, and M.L. Koszykowski, Chem. Phys. Lett. **133**, 513–516 (1987).
38. A.B. Dokuchaev, A.Yu. Pavlov, E.N. Stroganova, and M.V. Tonkov, Opt. Spektrosk. **60**, 947–952 (1986).
39. J.M. Hartman, L. Rosenman, and J. Taine, J. Quant. Spectrosc. Radiat. Transfer **40**, 93–99 (1988).
40. V. Menoux, R. Le Doucen, and C. Boulet, Appl. Optics **26**, 554–562 (1987).
41. B.H. Winter, S. Silverman, and W.S. Benedict, J. Quant. Spectrosc. Radiat. Transfer **4**, 527–537 (1964).
42. D.E. Burch, D.A. Gryvnak, R. H. Patty, and C.E. Bartky, J. Opt. Soc. Am. **59**, 267–280 (1960).
43. M.O. Bulanin, V.P. Bulychev, P.V. Granskii, et al., *Probl. Fiz. Atmos.*, 14–24, No. 13 (1976).

44. E.S. Kuznetsov, V.M. Osipov, and M.V. Podkladenko, Opt. Spektrosk. **38**, 36–38 (1975).
45. N.I. Moskalenko and O.V. Zotov, Izv. Akad. Nauk SSSR, Ser. FAO **13**, 488–498 (1977).
46. Yu.I. Baranov, M.O. Bulanin, and M.V.Tonkov, Opt. Spektrosk. **50**, 613–615 (1981).
41. Yu.I.Baranov and M.V.Tonkov, ibid. **57**, 242–247 (1984).
48. Kh. Sattarov and M.V. Tonkov, ibid. **54**, 944–946 (1983).
49. M.O. Bulanin, M.V. Tonkov, and N.N. Filippov, Can. J. Phys. **62**, 1306–1314 (1984).
50. G.A. Parker, R.L. Snow, and H.T. Pack, J. Chem. Phys. 64, 1668-1618 (1916).
51. G.D. Billing, Chem. Phys. Lett. **117**, 145–150 (1985).
52. G.A. Parker and R.T. Pack, J. Chem. Phys. **69**, 3268–3278 (1978).
53. L.D. Thomas, W.P. Kraemer, and G.H.F. Diercksen, Chem. Phys. **51**, 131–139 (1980).
54. M.V. Tonkov and N.N. Filippov, *Proceedings of the Seventh All–Union Symposium on Molecular Spectroscopy of High and Super–High Resolution,* Vol. **2**, 133–137, Tomsk (1986).
55. M.V. Tonkov and N.N. Filippov, *Proceedings of the Ninth All–Union Symposium on Molecular Spectroscopy of High and Super–High Resolution,* 64–66, Tomsk (1989).
56. N.N. Fillippov, ibid, p. 67.
57. A.P. Gal'tsev and V.V. Tsukanov, Opt. Spektrosk. **46**, 467–473 (1979).
58. L.I. Nesmelova, O.B. Rodimova, and S.D. Tvorogov, *The Spectral Line Shape and the Intermolecular Interaction* (Nauka, Novosibirsk, 1986), 147 pp.
59. W.S. Benedict, R. Herman, G.E. Moore, and S. Silverman, Astrophys. J. **135**, 277–297 (1962).
60. A.A. Vigasin, Opt. Atm. **2**, No. 10, 1069–1088 (1989).
61. L.I. Nesmelova, O.B. Rodimova,and S.D. Tvorogov, ibid. **1**, No. 4, 36–44 (1988).
62. J. Boissoles, V. Menoux, R. Le Doucen, et al., J. Chem. Phys. **91**, 2163–2171 (1989).